

Title: Mixed Session

Date: Jul 26, 2013 04:40 PM

URL: <http://pirsa.org/13070090>

Abstract:

THE HOLOGRAPHIC ENTROPY BOUND AND SEMI-CLASSICAL GRAVITATIONAL BACK REACTION.

Michael Reisenberger

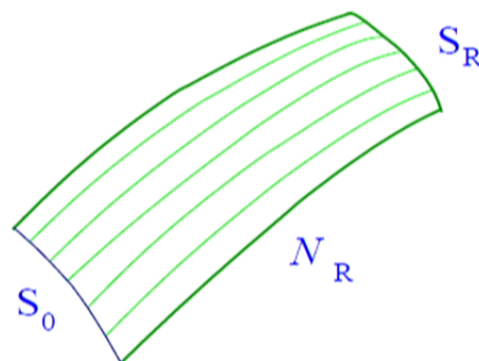
Universidad de la República, Uruguay

Loops '13, Waterloo, July 2013

BOUSSO'S FORM OF THE HOLOGRAPHIC ENTROPY BOUND

Beckenstein, 't Hooft, Susskind, Bousso

- **Null sheet** Hypersurface \mathcal{N}_R swept out in spacetime by future, null, normal geodesics (“generators”) emerging on one side of a spacelike 2-disk S_0 . Truncated before they cross or form caustics.
- Generators do not diverge at S_0 .

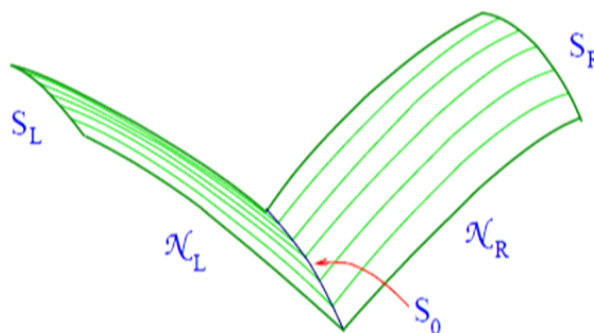


- Conjectured holographic entropy bound:

$$\text{Entropy on } \mathcal{N}_R \leq \frac{\text{Area}[S_0]}{4A_{\text{Planck}}}$$

WHAT IS "ENTROPY ON \mathcal{N}_R "?

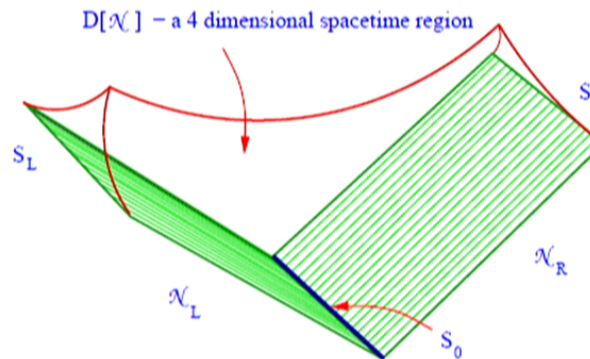
- When the field is in local equilibrium it is the flux of the entropy density vector through \mathcal{N}_R .
- In general, can define $\mathcal{N} = \mathcal{N}_L \cup \mathcal{N}_R$, the hypersurface swept out by the future, normal, null geodesics emerging from *both* sides of S_0 .



- If the generators are non-expanding on both sides of S_0 then the entropy bound implies

$$\text{Entropy}[\mathcal{N}] \leq \frac{\text{Area}[S_0]}{2A_{\text{Planck}}}$$

- Initial data on \mathcal{N} specifies solution in domain of dependence $D[\mathcal{N}]$, and we can define a phase space.

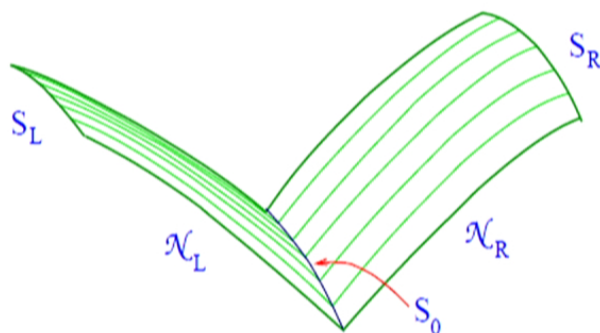


- The entropy of a macrostate \mathcal{N} is the logarithm of the number of compatible microstates.
- Normally the highest entropy thermodynamic macrostate of a system has essentially *all* microstates. This suggests

$$\dim H_{\mathcal{N}} \leq e^{\frac{A[S_0]}{2A_{\text{Planck}}}}$$

WHAT IS "ENTROPY ON \mathcal{N}_R "?

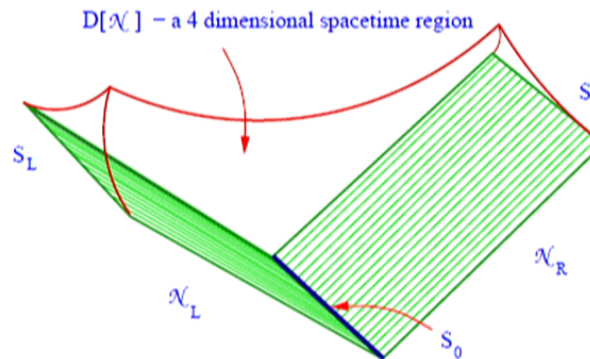
- When the field is in local equilibrium it is the flux of the entropy density vector through \mathcal{N}_R .
- In general, can define $\mathcal{N} = \mathcal{N}_L \cup \mathcal{N}_R$, the hypersurface swept out by the future, normal, null geodesics emerging from *both* sides of S_0 .



- If the generators are non-expanding on both sides of S_0 then the entropy bound implies

$$\text{Entropy}[\mathcal{N}] \leq \frac{\text{Area}[S_0]}{2A_{\text{Planck}}}$$

- Initial data on \mathcal{N} specifies solution in domain of dependence $D[\mathcal{N}]$, and we can define a phase space.

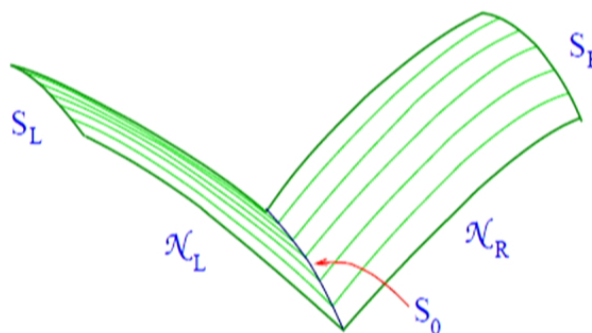


- The entropy of a macrostate \mathcal{N} is the logarithm of the number of compatible microstates.
- Normally the highest entropy thermodynamic macrostate of a system has essentially *all* microstates. This suggests

$$\dim H_{\mathcal{N}} \leq e^{\frac{A[S_0]}{2A_{\text{Planck}}}}$$

WHAT IS "ENTROPY ON \mathcal{N}_R "?

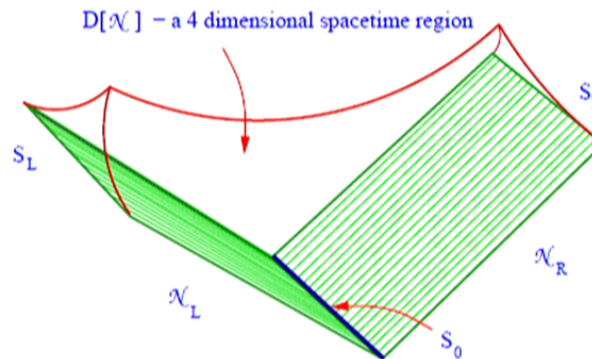
- When the field is in local equilibrium it is the flux of the entropy density vector through \mathcal{N}_R .
- In general, can define $\mathcal{N} = \mathcal{N}_L \cup \mathcal{N}_R$, the hypersurface swept out by the future, normal, null geodesics emerging from *both* sides of S_0 .



- If the generators are non-expanding on both sides of S_0 then the entropy bound implies

$$\text{Entropy}[\mathcal{N}] \leq \frac{\text{Area}[S_0]}{2A_{\text{Planck}}}$$

- Initial data on \mathcal{N} specifies solution in domain of dependence $D[\mathcal{N}]$, and we can define a phase space.



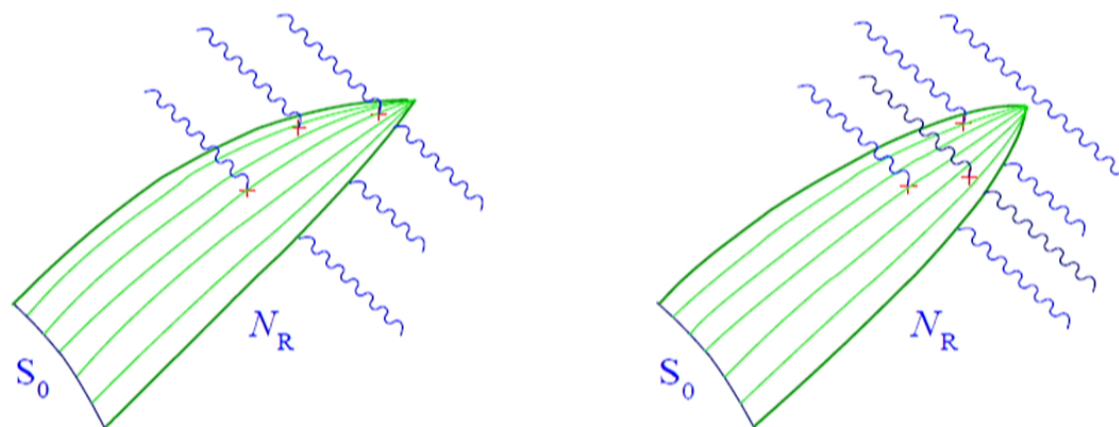
- The entropy of a macrostate \mathcal{N} is the logarithm of the number of compatible microstates.
- Normally the highest entropy thermodynamic macrostate of a system has essentially *all* microstates. This suggests

$$\dim H_{\mathcal{N}} \leq e^{\frac{A[S_0]}{2A_{\text{Planck}}}}$$

- Is this really true? Susskind (1995) suggested that it is a consequence of gravitational backreaction.
- Canonical GR on \mathcal{N} seems the ideal framework to check this rigorously. This is my long term project: [gr-qc/0703134](#) (2007), [gr-qc/0712.2541](#), PRL **101**, 211101 (2008), [gr-qc/1211.3880](#), CQG **30**, 155022 (2013). The theses of Rodrigo Eyheralde and Andreas Fuchs are also related to this.
- Here we will examine heuristic arguments for holography from backreaction.

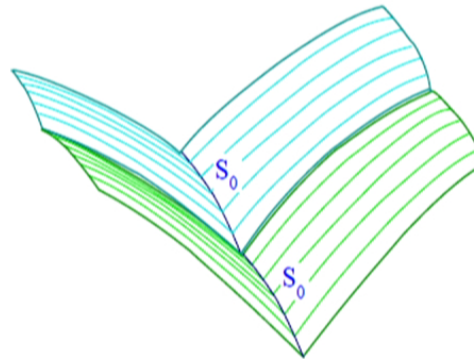
HOW CAN ONE UNDERSTAND THE HOLOGRAPHIC ENTROPY BOUND?

A simple picture: Suppose n quanta of a scalar field cross \mathcal{N}_R .



- Suppose we try to stuff one more quantum through \mathcal{N}_R . The generators converge more strongly and the quantum that was formerly at the tip of \mathcal{N}_R falls off. The number of quanta on \mathcal{N}_R remains n .

- Suppose we glue together two identical double null sheets \mathcal{N} , so they form a single double null sheet \mathcal{N}' with cross sectional area $2A[S_0]$.



- Points in the two \mathcal{N} s are spacelike to each other.
- Therefore, if the Hilbert space $\mathcal{H}_{\mathcal{N}}$ for data on \mathcal{N} has dimension N then the Hilbert space of \mathcal{N}' should have dimension N^2 .
- Thus the log of the dimensionality of $\mathcal{H}_{\mathcal{N}}$ should be extensive in $A[S_0]$.

A somewhat better picture, purely in terms of initial data on \mathcal{N} :

- Let θ be the expansion of the congruence of generators, and λ an affine parameter. Then

$$\frac{d\theta}{d\lambda} = -\frac{1}{2}\theta^2 - \sigma_{ab}\sigma^{ab} - 8\pi G\langle T_{\lambda\lambda}\rangle.$$

The shear σ will be ignored, it only makes the convergence of the generators faster, and we will assume that the null energy density $\langle T_{\lambda\lambda}\rangle$ has a uniform value τ on \mathcal{N}_R (and $0 = \theta = \lambda$ at S_0). Then $\theta = -2\sqrt{4\pi G\tau} \tan \sqrt{4\pi G\tau} \lambda$, and the generators form a caustic at

$$\lambda_{max} = \frac{\pi}{2} \frac{1}{\sqrt{4\pi G\tau}}.$$

The value $\bar{\lambda}$ of λ where the generators of \mathcal{N}_R are cut off must be less than λ_{max} .

- Suppose a field mode on \mathcal{N}_R , sinusoidal in λ , is excited with one quantum. Then $p_\lambda = \hbar k_\lambda$ but also $p_\lambda = \langle T_{\lambda\lambda}\rangle \bar{\lambda} A_{S_0} f$, with $f < 1$. Thus

$$\tau = \langle T_{\lambda\lambda}\rangle = \hbar k_\lambda / (\bar{\lambda} A_{S_0} f) > \hbar 2\pi m / (\bar{\lambda}^2 A_{S_0})$$

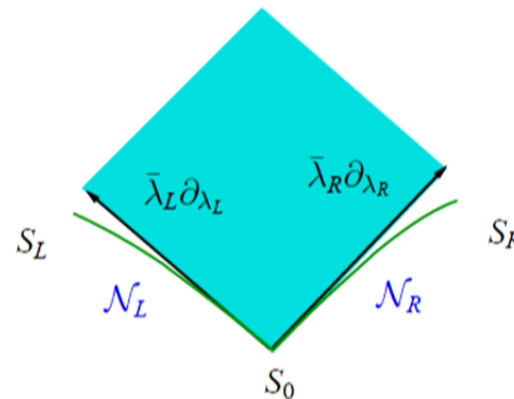
where m is the number of wavelengths of the mode along the generator.

- $\bar{\lambda} < \lambda_{max}$ then implies $m < A_{S_0}/(32G\hbar) = A_{S_0}/(32A_{Planck})$. If several modes m are occupied with n_m quanta in each then

$$\sum_m mn_m < A_{S_0}/(32A_{Planck}).$$

Does not show dimension of Hilbert space finite, since infinitely many modes on \mathcal{N} have the same m .

- But, if we apply the same reasoning to the other branch \mathcal{N}_L , and furthermore assume that $\bar{\lambda}_R \bar{\lambda}_L \partial_{\lambda_R} \cdot \partial_{\lambda_L} > A_{Planck}$ then only a finite subset of the Fock basis is allowed. Seems holographic!



- Can one do better using quantum field theory?

HOLOGRAPHIC PRINCIPLE AND QFT

Idea: Quantize initial data for scalar field on \mathcal{N} as in QFT on curved spacetime. $\langle T_{\lambda\lambda} \rangle$ causes focusing. Maybe only for some states of the field can metric initial data be found on \mathcal{N} such that the generators do not form caustics before leaving \mathcal{N} . Maybe the allowed states form a finite dimensional space. **Does this work?** There is an apparent counterexample: (Work with Rodrigo Eyheralde)

- Fock quantization of a free field: Linear system \implies choose linear (real) canonical coordinates Q_k, P_k and require corresponding operators satisfy $[\hat{Q}_k, \hat{P}_l] = i\hbar\delta_{kl}\mathbf{1}$.
- Equivalently set $\hat{a}_k = 1/\sqrt{2\hbar}(\hat{Q}_k + i\hat{P}_k)$ and require $[\hat{a}_k, \hat{a}_l^\dagger] = \delta_{kl}\mathbf{1}$.
- Define representation of operator algebra by requiring $\hat{a}_i|0\rangle = 0 \forall i$ for one state $|0\rangle$ and the Hilbert space is spanned by $|0\rangle, \hat{a}_i^\dagger|0\rangle, \hat{a}_j^\dagger\hat{a}_i^\dagger|0\rangle, \dots$
- Q_k, P_k define a metric, $g = \sum_k (Q_k^2 + P_k^2)$, on phase space that makes these coordinates orthonormal. g and symplectic 2-form Ω suffice to define the quantization uniquely.

- If vacuum satisfies μSC then $\langle \hat{T}_{ss} \rangle$ defined on a dense subspace of Fock space.
- Verch 1994 showed that Fock spaces with such vacua are “locally equivalent”. They cannot be distinguished via the expectation values of functions of the fields on an spacetime domain of compact closure.
- For these reasons (and others) μSC is required of “good vacua”.

So

- The vacuum in our does not quite satisfy μSC .
- When backreaction is included the field does not live on a fixed spacetime geometry, but the result suggests that some sort of positive energy requirement is essential for holography.

On the continuous limit of graphs

Jacobo Díaz Polo

in collaboration with: Iñaki Garay

Loops '13, Waterloo ON, July 2013



Motivation

One of the main predictions of quantum gravity is a discrete geometry at the fundamental level

In LQG, states given in terms of spin networks (based on graphs)

We expect continuous geometry to emerge in the semiclassical limit

Question: Is there any relation between a given graph and the compatible continuous geometries?

Hard problem in general, but there are some attempts in particular cases.

Bombelli, Corichi and Winkler (2004): Use Voronoi graphs

- Do they contain any geometric information encoded just in their abstract structure?

Motivation

One of the main predictions of quantum gravity is a discrete geometry at the fundamental level

In LQG, states given in terms of spin networks (based on graphs)

We expect continuous geometry to emerge in the semiclassical limit

Question: Is there any relation between a given graph and the compatible continuous geometries?

Hard problem in general, but there are some attempts in particular cases.

Bombelli, Corichi and Winkler (2004): Use Voronoi graphs

- Do they contain any geometric information encoded just in their abstract structure?

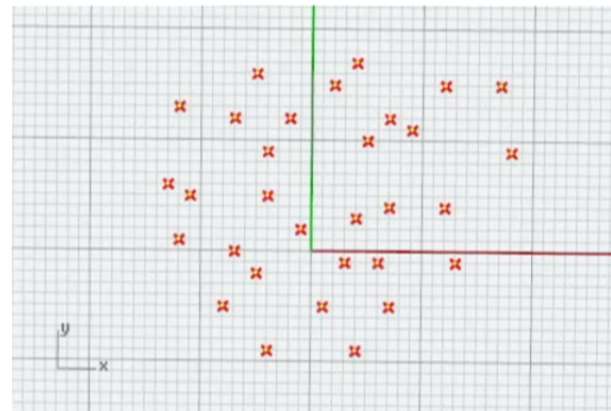
We want to ask: How well does it work?

What is a Voronoi diagram?

Seeds sprinkled on a (metric) space

Voronoi cell associated to a seed is the region of space closer to that seed than to any other one

Co-dimension N cells are equidistant to $N+1$ seeds

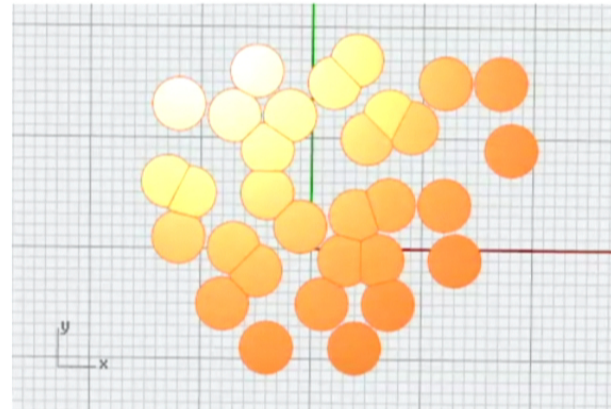


What is a Voronoi diagram?

Seeds sprinkled on a (metric) space

Voronoi cell associated to a seed is the region of space closer to that seed than to any other one

Co-dimension N cells are equidistant to N+1 seeds

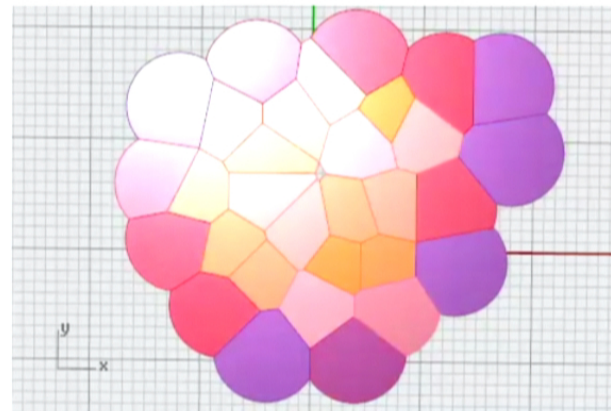


What is a Voronoi diagram?

Seeds sprinkled on a (metric) space

Voronoi cell associated to a seed is the region of space closer to that seed than to any other one

Co-dimension N cells are equidistant to N+1 seeds



What is a Voronoi diagram?

Seeds sprinkled on a (metric) space

Voronoi cell associated to a seed is the region of space closer to that seed than to any other one

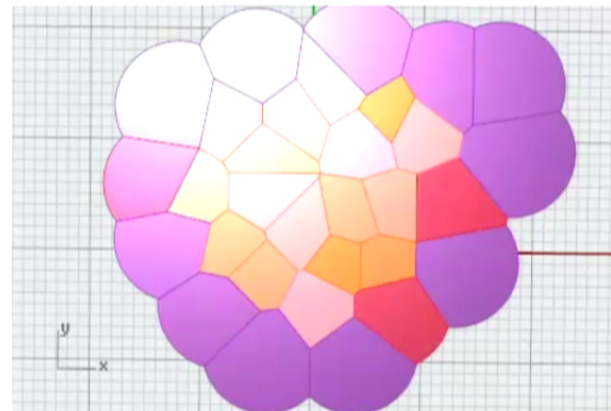
Co-dimension N cells are equidistant to $N+1$ seeds

In 2D

- Edges equidistant to 2 seeds
- Vertices equidistant to 3 seeds

In 3D

- Faces equidistant to 2 seeds
- Edges equidistant to 3 seeds
- Vertices equidistant to 4 seeds



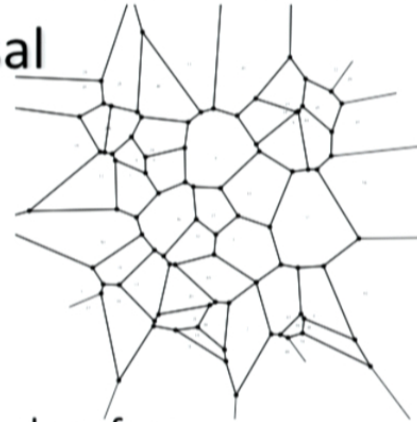
Dual of a Voronoi diagram is a triangulation: Delaunay Triangulation

Bombelli-Corichi-Winkler proposal

Annalen Phys. 14 (2005) 499–519 [arXiv:gr-qc/0409006]

We only consider here the 2D case:

- Randomly sprinkle a set of points on a given surface
- Construct the corresponding Voronoi diagram
- Throw away structures (cells) of dimension higher than 1
We are left with an abstract graph



Goal: Recover information about the original surface

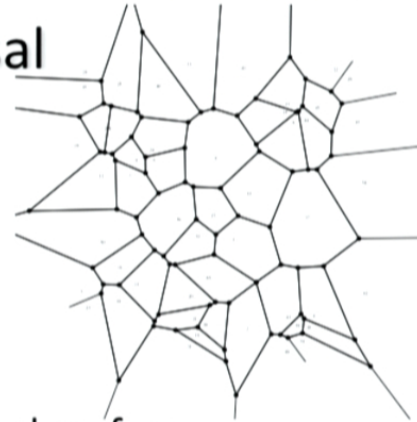
- Definition of 'plaquette': Closed loop such that contains the shortest path between any 2 vertices
- Additional input is needed to reconstruct the Voronoi diagram: Every edge shared by 2 faces.

Bombelli-Corichi-Winkler proposal

Annalen Phys. 14 (2005) 499–519 [arXiv:gr-qc/0409006]

We only consider here the 2D case:

- Randomly sprinkle a set of points on a given surface
- Construct the corresponding Voronoi diagram
- Throw away structures (cells) of dimension higher than 1
We are left with an abstract graph



Goal: Recover information about the original surface

- Definition of ‘plaquette’: Closed loop such that contains the shortest path between any 2 vertices
- Additional input is needed to reconstruct the Voronoi diagram: Every edge shared by 2 faces.

Compute the curvature

$$N_0 - N_1 + N_2 = \chi$$

$$N_1 = \frac{3}{2}N_0$$

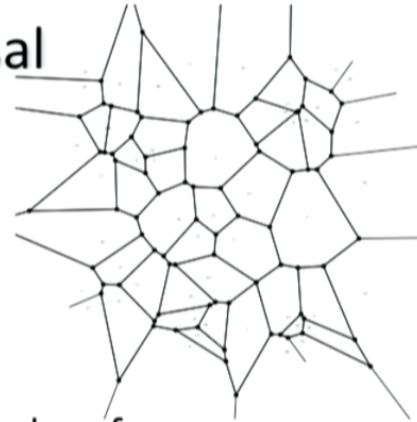
$$\langle N_1 \rangle = \frac{2N_1}{N_2}$$

Bombelli-Corichi-Winkler proposal

Annalen Phys. 14 (2005) 499-519 [arXiv:gr-qc/0409006]

We only consider here the 2D case:

- Randomly sprinkle a set of points on a given surface
- Construct the corresponding Voronoi diagram
- Throw away structures (cells) of dimension higher than 1
We are left with an abstract graph



Goal: Recover information about the original surface

- Definition of 'plaquette': Closed loop such that contains the shortest path between any 2 vertices
- Additional input is needed to reconstruct the Voronoi diagram: Every edge shared by 2 faces.

Compute the curvature

$$N_0 - N_1 + N_2 = \chi \quad \langle N_1 \rangle = 6 \left(1 - \frac{\chi}{N_2} \right) \quad \chi = \frac{1}{4\pi} \int_M R \, dV$$

$$N_1 = \frac{3}{2} N_0$$

$$\langle N_1 \rangle = \frac{2N_1}{N_2}$$

$$R = 4\pi \frac{N_2}{V} \left(1 - \frac{\langle N_1 \rangle}{6} \right)$$

Probing the discrete-to-continuous transition

Finding the appropriate size for a region of the graph such that:

- It is large enough to have good statistics
- It is small enough so that the constant-curvature approximation holds

Probing the discrete-to-continuous transition

Finding the appropriate size for a region of the graph such that:

- It is large enough to have good statistics
- It is small enough so that the constant-curvature approximation holds

BCW suggested:

- Choose an initial set of cells. Compute curvature (and standard deviation)



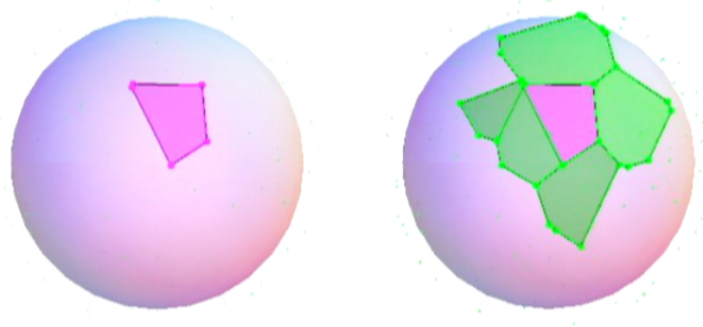
Probing the discrete-to-continuous transition

Finding the appropriate size for a region of the graph such that:

- It is large enough to have good statistics
- It is small enough so that the constant-curvature approximation holds

BCW suggested:

- Choose an initial set of cells. Compute curvature (and standard deviation)
- Consecutively add “layers” of increasing degree neighbor cells to the considered region



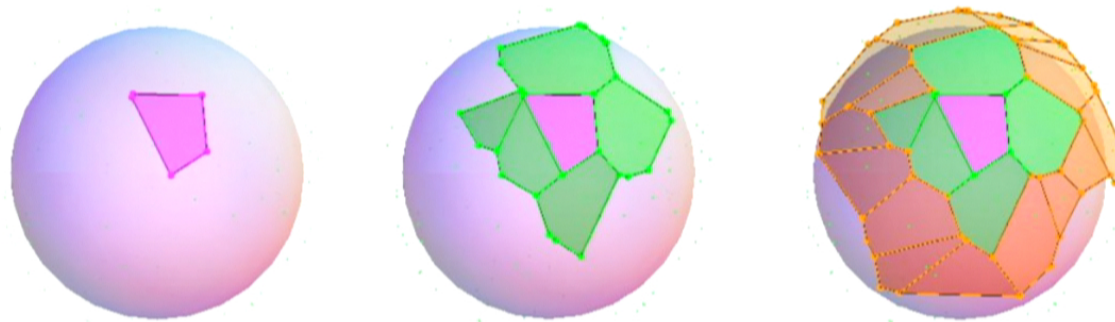
Probing the discrete-to-continuous transition

Finding the appropriate size for a region of the graph such that:

- It is large enough to have good statistics
- It is small enough so that the constant-curvature approximation holds

BCW suggested:

- Choose an initial set of cells. Compute curvature (and standard deviation)
- Consecutively add “layers” of increasing degree neighbor cells to the considered region



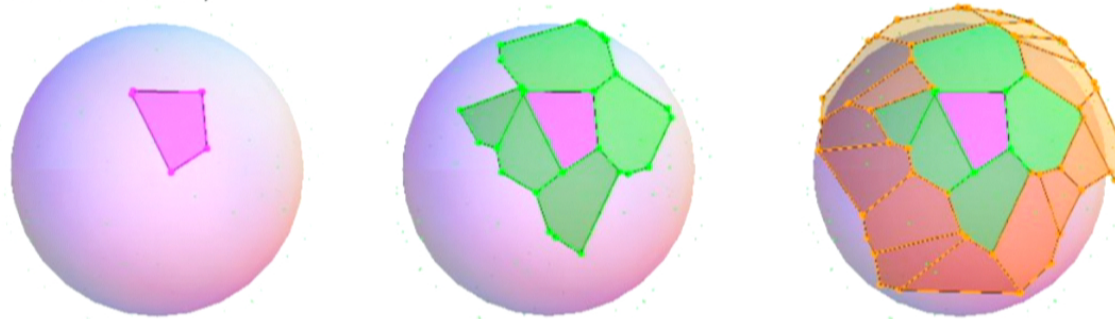
Probing the discrete-to-continuous transition

Finding the appropriate size for a region of the graph such that:

- It is large enough to have good statistics
- It is small enough so that the constant-curvature approximation holds

BCW suggested:

- Choose an initial set of cells. Compute curvature (and standard deviation)
- Consecutively add “layers” of increasing degree neighbor cells to the considered region
- Compute, at each step, the standard deviation and corresponding curvature
- Find the size for which dispersion is minimum (best compromise between good statistics and constant curvature).



Testing the BCW procedure

Start with the simplest case: A sphere

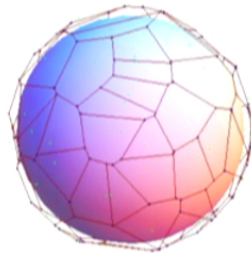
- No problem with making the region too large.
- Randomly sprinkle N points on the surface of a sphere
- Use standard computational algorithms to generate the corresponding Voronoi graph

Testing the BCW procedure

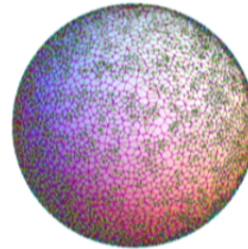
Start with the simplest case: A sphere

- No problem with making the region too large.
- Randomly sprinkle N points on the surface of a sphere
- Use standard computational algorithms to generate the corresponding Voronoi graph

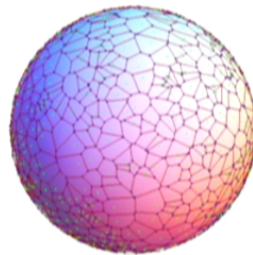
100 seeds



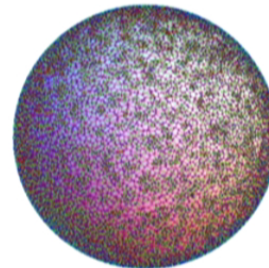
10K seeds



1K seeds



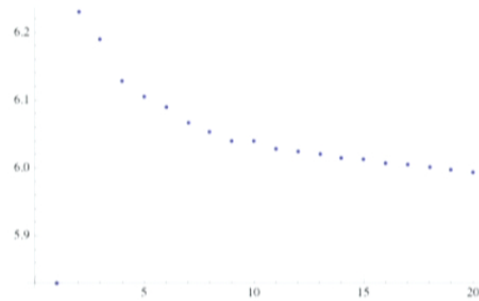
20K seeds



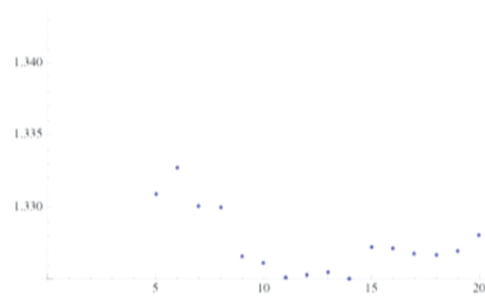
Testing the BCW procedure

1K seeds:

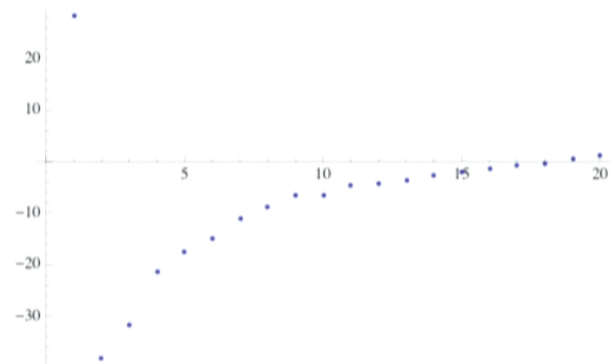
- Average number of sides of the faces



- Standard deviation



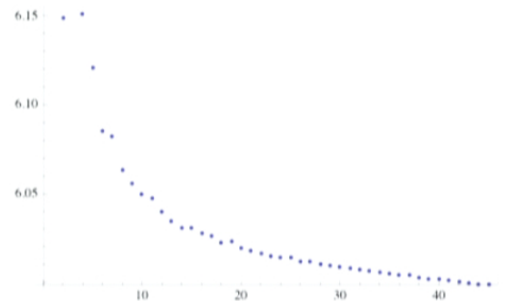
- Curvature



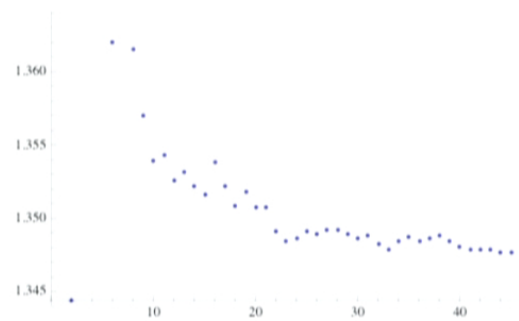
Testing the BCW procedure

5K seeds:

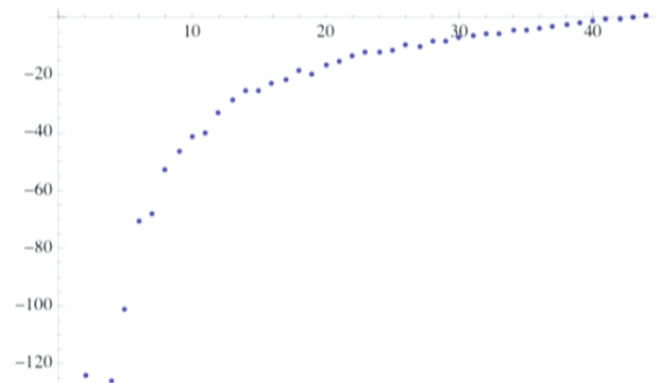
- Average number of sides of the faces



- Standard deviation



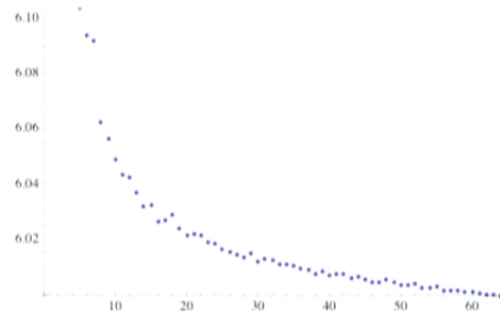
- Curvature



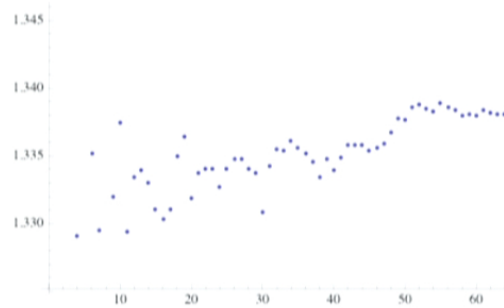
Testing the BCW procedure

10K seeds:

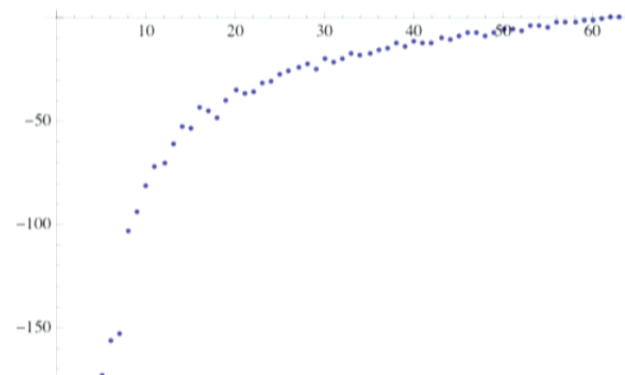
- Average number of sides of the faces



- Standard deviation



- Curvature



What went wrong?

Curvature does not stabilize to any value (though deviation does)

Even worse... curvature of a sphere appears to be negative!

- Except when the region considered is (almost) the whole sphere

Increasing the number of points (to “improve” statistics) does not seem to be of any help

What went wrong?

Curvature does not stabilize to any value (though deviation does)

Even worse... curvature of a sphere appears to be negative!

- Except when the region considered is (almost) the whole sphere

Increasing the number of points (to “improve” statistics) does not seem to be of any help

2 main questions arise:

- Do the assumptions made when deriving the curvature formula hold?
 - Something wrong with applying global (topological) properties to local regions?
 - Are we considering the right topology of things?
- Is the implementation procedure appropriate?

Disc topology and 'exact' formula

Actually, the regions we are considering have disc topology

- Some modifications to the relations between numbers of vertices and edges

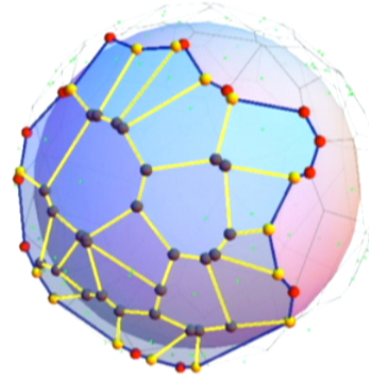
Disc topology and 'exact' formula

Actually, the regions we are considering have disc topology

- Some modifications to the relations between numbers of vertices and edges

$$N_0 - N_1 + N_2 = \chi$$

$$\langle N_1 \rangle = \frac{2N_1^{(i)} + N_1^{(e)}}{N_2}$$



Disc topology and 'exact' formula

Actually, the regions we are considering have disc topology

- Some modifications to the relations between numbers of vertices and edges

$$N_0 - N_1 + N_2 = \chi$$

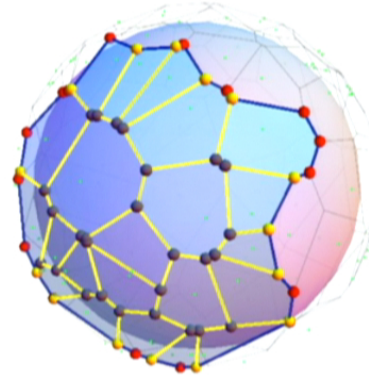
$$\langle N_1 \rangle = \frac{2N_1^{(i)} + N_1^{(e)}}{N_2}$$

$$N_1^{(i)} = \frac{3}{2}N_0^{(i)} + \frac{1}{2}N_0^{(e)}$$

$$N_1^{(e)} = N_0^{(e)} + N_0^{(o)}$$

- New boundary term:

$$\langle N_1 \rangle = 6 \left(1 - \frac{\chi}{N_2} \right) + \frac{N_0^{(o)} - N_0^{(e)}}{N_2}$$



Disc topology and 'exact' formula

Actually, the regions we are considering have disc topology

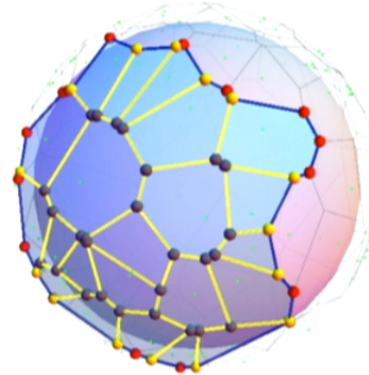
- Some modifications to the relations between numbers of vertices and edges

$$N_0 - N_1 + N_2 = \chi$$

$$\langle N_1 \rangle = \frac{2N_1^{(i)} + N_1^{(e)}}{N_2}$$

$$N_1^{(i)} = \frac{3}{2}N_0^{(i)} + \frac{1}{2}N_0^{(e)}$$

$$N_1^{(e)} = N_0^{(e)} + N_0^{(o)}$$



- New boundary term:

$$\langle N_1 \rangle = 6 \left(1 - \frac{\chi}{N_2} \right) + \frac{N_0^{(o)} - N_0^{(e)}}{N_2}$$

Gauss-Bonnet theorem also acquires an additional boundary term

$$\chi = \frac{1}{4\pi} \int_M R \, dV + \frac{1}{2\pi} \int_{\partial M} k_g \, ds$$

Disc topology and 'exact' formula

We can re-derive the analogous formula for the disc case:

$$\chi = \frac{1}{4\pi} \int_M R \, dV + \frac{1}{2\pi} \int_{\partial M} k_g \, ds = N_2 \left(1 - \frac{\langle N_1 \rangle}{6} \right) + \frac{N_0^{(o)} - N_0^{(e)}}{6}$$

- For a constant curvature region:

$$\chi = R \frac{V}{4\pi} + B.T. = N_2 \left(1 - \frac{\langle N_1 \rangle}{6} \right) + \frac{N_0^{(o)} - N_0^{(e)}}{6}$$

Disc topology and 'exact' formula

We can re-derive the analogous formula for the disc case:

$$\chi = \frac{1}{4\pi} \int_M R \, dV + \frac{1}{2\pi} \int_{\partial M} k_g \, ds = N_2 \left(1 - \frac{\langle N_1 \rangle}{6} \right) + \frac{N_0^{(o)} - N_0^{(e)}}{6}$$

- For a constant curvature region:

$$\chi = R \frac{V}{4\pi} + B.T. = N_2 \left(1 - \frac{\langle N_1 \rangle}{6} \right) + \frac{N_0^{(o)} - N_0^{(e)}}{6}$$

We need to split bulk and boundary to compute the curvature

- First term depends on 'bulk variables' and coincides with the bulk term for a full sphere
- Second term depends on 'boundary' variables and disappears for the full sphere
- Therefore, there seems to be a natural splitting in our formula
- But... assuming that splitting is equivalent to use the same formula we had before

Disc topology and 'exact' formula

We can re-derive the analogous formula for the disc case:

$$\chi = \frac{1}{4\pi} \int_M R \, dV + \frac{1}{2\pi} \int_{\partial M} k_g \, ds = N_2 \left(1 - \frac{\langle N_1 \rangle}{6} \right) + \frac{N_0^{(o)} - N_0^{(e)}}{6}$$

- For a constant curvature region:

$$\chi = R \frac{V}{4\pi} + B.T. = N_2 \left(1 - \frac{\langle N_1 \rangle}{6} \right) + \frac{N_0^{(o)} - N_0^{(e)}}{6}$$

We need to split bulk and boundary to compute the curvature

- First term depends on 'bulk variables' and coincides with the bulk term for a full sphere
- Second term depends on 'boundary' variables and disappears for the full sphere
- Therefore, there seems to be a natural splitting in our formula
- But... assuming that splitting is equivalent to use the same formula we had before

Either we find a different splitting or we are in the exact same case

- We haven't found any well-motivated alternative splitting

Problems with the implementation procedure?

Is there something wrong with the way we choose the region?

Why Your Friends Have More Friends than You Do¹

Scott L. Feld

State University of New York at Stony Brook

It is reasonable to suppose that individuals use the number of friends that their friends have as one basis for determining whether they, themselves, have an adequate number of friends. This article shows that, if individuals compare themselves with their friends, it is likely that most of them will feel relatively inadequate. Data on friendship drawn from James Coleman's (1961) classic study *The Adolescent Society* are used to illustrate the phenomenon that most people have fewer friends than their friends have. The logic underlying the phenomenon is mathematically explored, showing that the mean number of friends of friends is always greater than the mean number of friends of individuals. Further analysis shows that the proportion of individuals who have fewer friends than the mean number of friends their own friends have is affected by the exact arrangement of friendships in a social network. This disproportionate experiencing of friends with many friends is related to a set of abstractly similar "class size paradoxes" that includes such diverse phenomena as the tendencies for college students to experience the mean class size as larger than it actually is and for people to experience beaches and parks as more crowded than they usually are.

American Journal of Sociology, Vol. 96, No. 6 (May, 1991), pp. 1464-1477

Problems with the implementation procedure?

Is there something wrong with the way we choose the region?

Bigger cells have a higher chance of entering the region earlier

The Anatomy of the Facebook Social Graph

Johan Ugander^{1,2*}, Brian Karrer^{1,3*}, Lars Backstrom¹, Cameron Marlow^{1†}

1 Facebook, Palo Alto, CA, USA

2 Cornell University, Ithaca, NY, USA

3 University of Michigan, Ann Arbor, MI, USA

* These authors contributed equally to this work.

† Corresponding author: cameron@fb.com

Abstract

We study the structure of the social graph of active Facebook users, the largest social network ever analyzed. We compute numerous features of the graph including the number of users and friendships, the degree distribution, path lengths, clustering, and mixing patterns. Our results center around three main observations. First, we characterize the global structure of the graph, determining that the social network is nearly fully connected, with 99.91% of individuals belonging to a single large connected component, and we confirm the ‘six degrees of separation’ phenomenon on a global scale. Second, by studying the average local clustering coefficient and degeneracy of graph neighborhoods, we show that while the Facebook graph as a whole is clearly sparse, the graph neighborhoods of users contain surprisingly dense structure. Third, we characterize the assortativity patterns present in the graph by studying the basic demographic and network properties of users. We observe clear degree assortativity and characterize the extent to which ‘your friends have more friends than you’. Furthermore, we observe a strong effect of age on friendship preferences as well as a globally modular community structure driven by nationality, but we do not find any strong gender homophily. We compare our results with those from smaller social networks and find mostly, but not entirely, agreement on common structural network characteristics.

Introduction

The emergence of online social networking services over the past decade has revolutionized how social scientists study the structure of human relationships [1]. As individuals bring their social relations online, the focal point of the internet is evolving from being a network of documents to being a network of people, and previously invisible social structures are being captured at tremendous scale and with unprecedented detail. In this work, we characterize the structure of the world’s largest online social network, Facebook, in an effort to advance the state of the art in the empirical study of social networks.

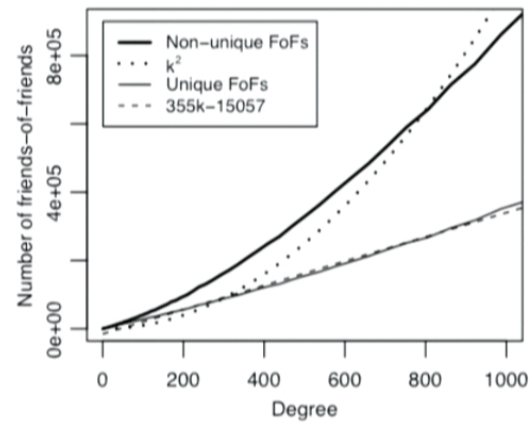
In its simplest form, a social network contains individuals as vertices and edges as relationships between vertices [2]. This abstract view of human relationships, while certainly limited, has been very useful for

Problems with the implementation procedure?

Is there something wrong with the way we choose the region?

Bigger cells have a higher chance of entering the region earlier

- Is this effect increasing the average and messing up the curvature “measurement”?



Problems with the implementation procedure?

Is there something wrong with the way we choose the region?

Bigger cells have a higher chance of entering the region earlier

- Is this effect increasing the average and messing up the curvature “measurement”?

How can we try to avoid it?

- If everyone had the same number of “friends” (uniform distribution), the average would be the same for everyone
- The vertices of our Voronoi graphs are all 3-valent, therefore they all have the same connectivity
- Use the ‘neighborhood subgraph’ to define the region (instead of the cells)

Problems with the implementation procedure?

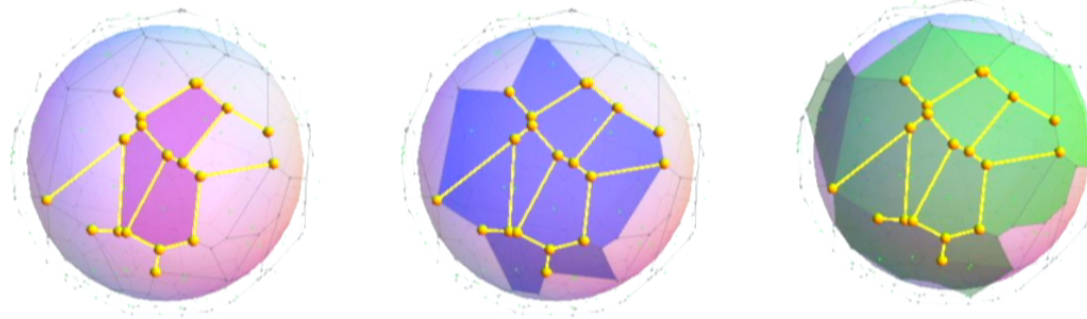
Is there something wrong with the way we choose the region?

Bigger cells have a higher chance of entering the region earlier

- Is this effect increasing the average and messing up the curvature “measurement”?

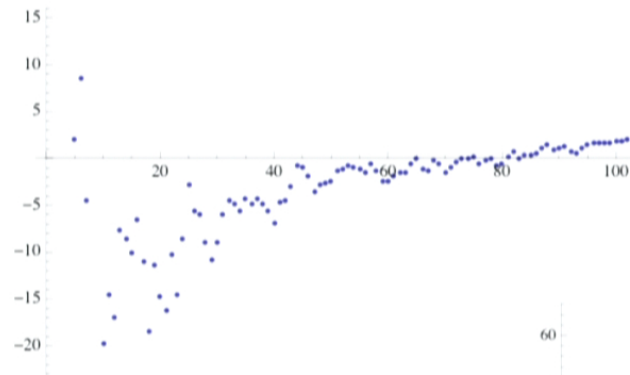
How can we try to avoid it?

- If everyone had the same number of “friends” (uniform distribution), the average would be the same for everyone
- The vertices of our Voronoi graphs are all 3-valent, therefore they all have the same connectivity
- Use the ‘neighborhood subgraph’ to define the region (instead of the cells)
- Still, open question: How to determine which cells are “selected” by a certain subgraph?



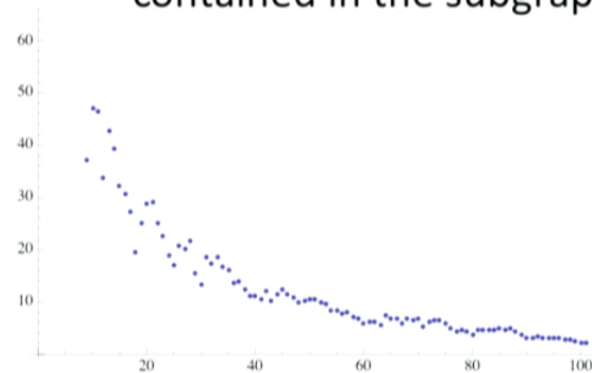
Using the neighborhood subgraph

Cells with at least half of their vertices contained in subgraph



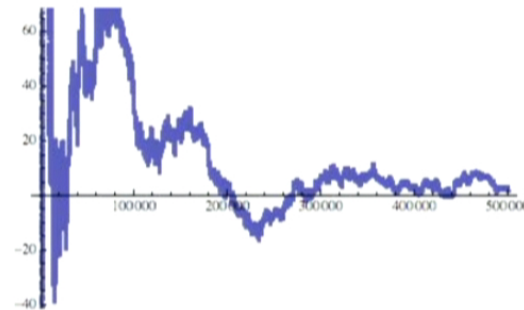
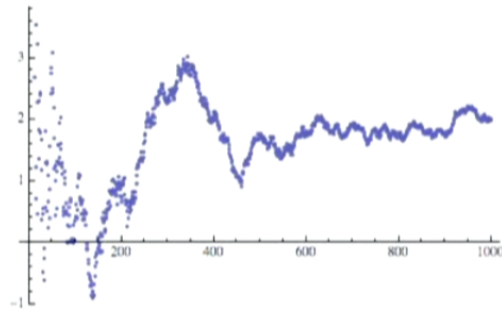
- The effect of the region choice is huge
- A small change sends curvatures from positive to negative

Cells with all their vertices contained in the subgraph



One last, desperate attempt

Choosing a random subset of cells



Seems to 'stabilize', but only after considering about half the total number of cells

- That doesn't improve with a finer graph

Moreover, the deviations get worse for finer graphs!!!

Adding more cells does not seem to improve the statistics at all.

What is really going on?

If we define: $N_1 = \frac{N_2 \langle N_1 \rangle}{2} = \frac{6N_2}{2} + L_0$ then $L_0 = -6$

- The 'deficit of edges' for the whole sphere is constant, independent of the number of faces.
- This is a direct consequence of using topological quantities.
- What is relevant is what 'fraction' of a sphere is contained in the considered region, rather than the number of faces in it (how fine the graph is).

As a consequence:

- The curvature we are trying to measure scales as: $R \sim \rho (6 - \langle N_1 \rangle) \sim \rho \frac{1}{N_2}$
- Whereas the deviation goes with: $\sigma_R \sim \frac{1}{\sqrt{N_2}}$
- Therefore, the relative error increases as $\frac{1}{\sqrt{N_2}}$ when we refine the graph! :(

BCW proposal is a first step to tackle a very interesting question

- It exploits an interesting idea and seems to be conceptually consistent
- But, after all, this way of applying global, topological concepts to local computations does not seem to be a very useful approach in practice.

We need to keep working on new proposals! :)

Conclusions

In the problem of finding a semiclassical, continuous limit of LQG, the transition from discrete to smooth geometries could play an important role.

More work is needed in order to obtain interesting relations between the abstract graph structure and the compatible geometries.

Furthermore, unexpected issues arise, that might overshadow the same “geometric” quantities one is interested on measuring.

We have seen here that the criteria used to select a graph region can affect decisively the averages one is trying to estimate.

These (or similar) issues could reproduce when trying to make a connection between a spin network state and a smooth geometry.

We do not have, at this point, a satisfactory solution for these issues, in particular the selection of a finite region.

However, it is worth pointing out that these issues are present, and future attempts to work further in the discrete-to-continuous transition should take them into account.



Snyder spacetime: a novel view

Valerio Astuti

"La Sapienza" University of Rome

Loops 13 Conference
Perimeter Institute, July 26 2013



Click on Sign to add text
and place signature on a
PDF File.

This talk is based on a joint work with Giovanni Amelino-Camelia.

Part of the work has been under the hospitality of the Perimeter Institute.



Click on Sign to add text
and place signature on a
PDF File.

Introduction

- Non commutative spacetimes $[x^\mu, x^\nu] = i\ell F^{\mu\nu}(x)$
- Covariant quantum mechanics¹ $[p_\mu, q^\nu] = i\delta_\mu^\nu$
- Application to Snyder spacetime

¹Reisenberger, Rovelli 2002



Noncommutative coordinates

$$[x^\mu, x^\nu] = i\ell F^{\mu\nu}(x, p)$$

- They are thought to implement quantum properties of spacetime
- They can provide a physical cut-off for field theories
- Possibly effective theory to a more fundamental quantum theory of gravity



Snyder spacetime

$$[x^\mu, x^\nu] = i\ell^2 M^{\mu\nu} = i\ell^2 (x^\mu p^\nu - x^\nu p^\mu)$$

- First proposed noncommutative spacetime
- Preserves Lorentz invariance
- Lattice space structure

Discreteness of Snyder space

- The operators

$$M^{ij}, \quad M^{i4} = \frac{x^i}{\ell}, \quad M^{AB} = -M^{BA}$$

form an $SO(4)$ subalgebra

$$-i[M^{AB}, M^{CD}] = \delta^{AC} M^{BD} - \delta^{BC} M^{AD} + \\ -\delta^{AD} M^{BC} + \delta^{BD} M^{AC}$$

- This algebra can be factorized in the product of two copies of $SU(2)$ with the same casimir, and has representations with basis $|j, m_A, m_B\rangle$
- We can diagonalize one coordinate, say x^3 , and obtain the spectrum:

$$x^3 |j, m_A, m_B\rangle = \ell(m_A - m_B) |j, m_A, m_B\rangle$$



Noncommutative coordinates

$$[x^\mu, x^\nu] = i\ell F^{\mu\nu}(x, p)$$

- They are thought to implement quantum properties of spacetime
- They can provide a physical cut-off for field theories
- Possibly effective theory to a more fundamental quantum theory of gravity

Kinematical space

Spacetime coordinates are observables in a quantum mechanical Hilbert space $L^2(\mathbb{R}^2, dq^0 dq^1)$:

- Canonical commutation relations $[p_\mu, q^\nu] = i\delta_\mu^\nu$
- States are (integrable) functions $\psi(q^0, q^1)$ describing probabilities of finding a particle in a spacetime region
- Provide a good environment to represent nontrivial commutation relations for coordinates
- There is no dynamics!



Symmetries and Dynamics

We can impose dynamics on such a space imposing the constraint

$$H(p)\psi = 0$$

H being the casimir of the symmetry algebra:

- Examples:

$$H = p_0 - \frac{\vec{p}^2}{2m} \quad \text{Galilean quantum mechanics}$$

$$H = p_0^2 - \vec{p}^2 - m^2 \quad \text{Relativistic quantum mechanics}$$



Kinematical space

Spacetime coordinates are observables in a quantum mechanical Hilbert space $L^2(\mathbb{R}^2, dq^0 dq^1)$:

- Canonical commutation relations $[p_\mu, q^\nu] = i\delta_\mu^\nu$
- States are (integrable) functions $\psi(q^0, q^1)$ describing probabilities of finding a particle in a spacetime region
- Provide a good environment to represent nontrivial commutation relations for coordinates
- There is no dynamics!

Physical space

- To implement the constraint we change the scalar product:

$$\langle \psi | \phi \rangle_P = \int dp \delta(H) \bar{\psi}(p) \phi(p)$$

with ψ, ϕ elements of the kinematical space

- Now the only physical observables are the self-adjoint operators with respect to the **physical** scalar product
- In particular a combination of kinematic observables must commute with the constraint to be a physical observable



Symmetries and Dynamics

We can impose dynamics on such a space imposing the constraint

$$H(p)\psi = 0$$

H being the casimir of the symmetry algebra:

- Examples:

$$H = p_0 - \frac{\vec{p}^2}{2m} \quad \text{Galilean quantum mechanics}$$

$$H = p_0^2 - \vec{p}^2 - m^2 \quad \text{Relativistic quantum mechanics}$$

Physical coordinates

Physical coordinates, describing particles, are not the observables in kinematical phase space but observables in the **physical space**:

- Heisenberg coordinates $x^i = q^i - v^i q^0$
- Newton-Wigner operator $A^i = q^i - \frac{p^i}{p^0} q^0 + \frac{p^i}{2p_0^2}$
- Generalized N-W operators² $\chi^\mu = q^\mu - \frac{p^\mu}{p \cdot v} q \cdot v + h.c.$

²Freidel, Girelli, Livine 2007



Representation of Snyder Coordinates

Snyder himself provided a representation of his coordinates:

$$x^\mu = q^\mu - \ell^2 p^\mu (p \cdot q)$$

But this representation lives in the kinematical hilbert space, we cannot describe dynamics!

Snyder observables

We have to impose a constraint on the Snyder representation to obtain the physical coordinates

- Deformed Newton-Wigner operator:

$$A_{\ell}^i = x^i - \frac{p^i}{p^0} x^0 + \frac{p^i}{2p_0^2}$$

- Generalized deformed N-W operators:

$$\chi_{\ell}^{\mu} = x^{\mu} - \frac{p^{\mu}}{p \cdot v} x \cdot v + h.c.$$



Triviality of Snyder physical coordinates

All ℓ corrections **drop out** from physical coordinates!

$$\begin{aligned}
 \chi_{\ell}^{\mu} &= x^{\mu} - \frac{p^{\mu}}{p \cdot v} x \cdot v + h.c. = \\
 &= q^{\mu} - \ell^2 p^{\mu} (p \cdot q) - \frac{p^{\mu}}{p \cdot v} (q^{\nu} - \ell^2 p^{\nu} (p \cdot q)) v_{\nu} + h.c. = \\
 &= q^{\mu} - \frac{p^{\mu}}{p \cdot v} (q \cdot v) + h.c. = \chi^{\mu}
 \end{aligned}$$

Snyder observables

We have to impose a constraint on the Snyder representation to obtain the physical coordinates

- Deformed Newton-Wigner operator:

$$A_{\ell}^i = x^i - \frac{p^i}{p^0} x^0 + \frac{p^i}{2p_0^2}$$

- Generalized deformed N-W operators:

$$\chi_{\ell}^{\mu} = x^{\mu} - \frac{p^{\mu}}{p \cdot v} x \cdot v + h.c.$$

Generic spacetime functions

Given a general functions of kinematical phase space $f(p, q)$ for it to commute with the constraint it has to be function of the boost generators:

$$f(p, q) = \hat{f}(p, M)$$

$$M^{\mu\nu} = q^\mu p^\nu - q^\nu p^\mu$$

Without a deformation of the symmetry group you cannot have a deformation of spacetime variables!



Conclusions

- Representations of noncommutative spacetimes are usually in the kinematical space, and have problems introducing dynamics
- We should consider the physical observables, obtained after the imposition of the constraint
- Snyder spacetime, not deforming the Lorentz group, has trivial physical spacetime sector, even if the kinematical sector is deformed!
- Discreteness of spacetime observables in the kinematical hilbert space **does not necessarily imply** any discreteness in the physical spacetime variables!



Click on Sign to add text
and place signature on a
PDF File.

References

- G.Amelino-Camelia, V.Astuti, G.Rosati, "Relative locality in a quantum spacetime and the pregeometry of k-Minkowski", arxiv:1206.3805
- G.Amelino-Camelia, V.Astuti, G.Rosati, "Predictive description of Planck-scale-induced spacetime fuzziness", Phys.Rev. D87 (2013) 084023
- G.Amelino-Camelia, V.Astuti, "A modern reassessment of Snyder's noncommutative spacetime", soon on arxiv!

Discrete spatial geometry in real connection formulation



A hallmark of loop quantum gravity

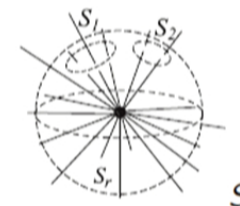
$$\text{Area}^*: \hat{A}_S |s\rangle = a |s\rangle$$

$$a = \ell_P^2 \sum_{n=1}^N \sqrt{j_n(j_n + 1)}$$



$$\text{Angle}^\dagger: \hat{\theta} |s\rangle = \theta |s\rangle$$

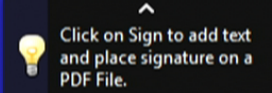
$$\theta = \arccos \left(\frac{j_r(j_r + 1) - j_1(j_1 + 1) - j_2(j_2 + 1)}{2 [j_1(j_1 + 1) j_2(j_2 + 1)]^{1/2}} \right)$$



* Rovelli, Smolin Nuc. Phys. B 422 (1995) 593; Ashtekar, Lewandowski Class. Quant. Grav. 14 (1997) A43

† SM Class. Quant. Grav. 16 (1999) 3859 gr-qc/9905019

Quantum Geometry Phenomenology



If physically correct, these quanta of spatial geometry will be observationally manifest.

- How? In what manner? Through modified dispersion relations (MDR)?
- Specifically which steps in the quantization yield observational effects (even in principle)

Discrete spatial geometry in real connection formulation



A hallmark of loop quantum gravity

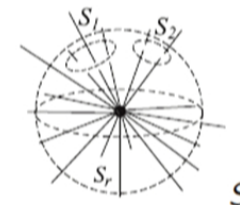
$$\text{Area}^*: \hat{A}_S |s\rangle = a |s\rangle$$

$$a = \ell_P^2 \sum_{n=1}^N \sqrt{j_n(j_n + 1)}$$



$$\text{Angle}^\dagger: \hat{\theta} |s\rangle = \theta |s\rangle$$

$$\theta = \arccos \left(\frac{j_r(j_r + 1) - j_1(j_1 + 1) - j_2(j_2 + 1)}{2 [j_1(j_1 + 1) j_2(j_2 + 1)]^{1/2}} \right)$$



* Rovelli, Smolin Nuc. Phys. B 422 (1995) 593; Ashtekar, Lewandowski Class. Quant. Grav. 14 (1997) A43

† SM Class. Quant. Grav. 16 (1999) 3859 gr-qc/9905019

Plane gravitational waves: Exact solution



An example “simple enough system” retaining local degrees of freedom to study possible effects

Metric of plane wave

$$ds^2 = -dt^2 + L^2 e^{2\beta} dx^2 + L^2 e^{-2\beta} dy^2 + dz^2.$$

L and β are functions of $u := t - z$ (or, $v := t + z$, but not both!).
Einstein's equations become simply

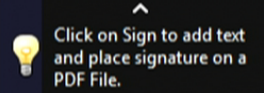
$$\partial_u^2 L + (\partial_u \beta)^2 L = 0.$$

The “background factor” L evolves according to the (free) “wave factor” β acting as a “time”-dependent angular frequency.

Misner, Thorne, Wheeler Gravitation

J. Ehlers and W. Kundt, L. Witten, ed. Gravitation: An Introduction to Current Research

Plane gravitational waves: On loop quantization

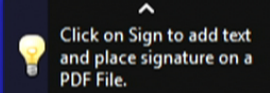


Preparation for loop quantization

Done so far:

- Planar symmetric space-times reduced to single-way propagation with a (non-diffeo invariant) constraint.
Results in non-local Dirac brackets [Hinterleitner, SM *Phys. Rev. D* **83** (2011) 044034 arXiv:1006.4146]
- Reformulated constraints into first class system
Now model accessible to LQG techniques [Hinterleitner, SM *Class. Quantum Grav.* **29** (2012) 065019 arXiv:1106.1448]
- Loop quantization - Work in progress

Plane gravitational waves: Classical system



The space-time metric is

$$ds^2 = -N^2 dt^2 + \mathcal{E} \frac{E^y}{E^x} dx^2 + \mathcal{E} \frac{E^x}{E^y} dy^2 + \frac{E^x E^y}{\mathcal{E}} dz^2$$

with all variables functions of z and t . With symmetry reduction the phase space (A_a^i, E^{bj}) become an 8 dimensional phase space $\{(K_a, E^a), (\mathcal{A}, \mathcal{E}), (\eta, P)\}$ with relations

$$\begin{aligned} \{K_a(z), E^b(z')\} &= \kappa \delta_a^b \delta(z - z'), & \{\mathcal{A}(z), \mathcal{E}(z')\} &= \kappa \delta(z - z'), \\ \{\eta(z), P(z')\} &= \kappa \gamma \delta(z - z') \end{aligned}$$

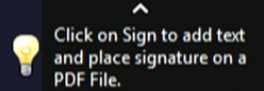
where a, b, \dots are x or y , κ is the gravitational constant times a fiducial area and γ is the Barbero-Immirzi parameter. K is proportional to the connection A .

Banerjee and Date, 0712.0683 and 0712.0687

Bojowald and Swiderski gr-qc/ 0511108



Plane gravitational waves: Classical system



In reduced system constraints are (primes ' denote ∂_z)

- Gauss

$$G = \frac{1}{\kappa\gamma} (\mathcal{E}' + P)$$

- Diffeo

$$C = \frac{1}{\kappa} \left[K'_x E^x + K'_y E^y - \mathcal{E}' \mathcal{A} + \frac{\eta'}{\gamma} P \right]$$

- Hamiltonian

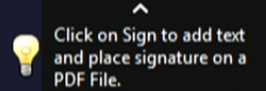
$$H = -\frac{1}{\kappa\sqrt{\mathcal{E}E^xE^y}} \left[E^x K_x E^y K_y + (E^x K_x + E^y K_y) \mathcal{E} \left(\mathcal{A} + \frac{\eta'}{\gamma} \right) - \frac{1}{4} \mathcal{E}'^2 - \mathcal{E} \mathcal{E}'' \right. \\ \left. - \frac{1}{4} \mathcal{E}^2 \left[\left(\ln \frac{E^y}{E^x} \right)' \right]^2 + \frac{1}{2} \mathcal{E} \mathcal{E}' (\ln E^x E^y)' \right] - \frac{\kappa}{4\sqrt{\mathcal{E}E^xE^y}} G^2 - \gamma \left(\sqrt{\frac{\mathcal{E}}{E^xE^y}} G \right)'.$$

- Right-moving constraint from existence of null Killing field

$$U_+ = E^x K_x + E^y K_y - \mathcal{E}'$$



Plane gravitational waves: Classical system



With first-class algebra

$$\begin{aligned}\{U_+[f], G[g]\} &= 0, \\ \{U_+[f], C[g]\} &= -\frac{1}{\kappa} U_+[f'g] \approx 0, \\ \{U_+[f], H[g]\} &= \frac{1}{\kappa} U_+ \left[\sqrt{\frac{\mathcal{E}}{E^x E^y}} f'g \right] - H[fg] \approx 0.\end{aligned}$$

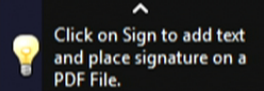
and GR

$$\begin{aligned}\{G[f], G[g]\} &= \{G[f], H[g]\} = 0, & \{G[f], C[g]\} &= -G[f'g], \\ \{C[f], C[g]\} &= C[fg' - f'g], & \{C[f], H[g]\} &= H[fg'], \\ \{H[f], H[g]\} &= C \left[(fg' - f'g) \frac{\mathcal{E}}{E^x E^y} \right].\end{aligned}$$

Algebra (still) has structure functions.



Plane gravitational waves: Classical system



For “no-wave” state or flat space we could impose “right”- U_+ and “left”-moving

$$U_- = E^x K_x + E^y K_y + \mathcal{E}'$$

constraints. Alternatively we could, and will, use

$$\mathcal{K} := XE^x + YE^y = 0 \text{ and } \mathcal{E}' = 0.$$

These can be expressed as the vanishing of the “time” rate of change of the cross sectional “area” $g_{xx} \cdot g_{yy} = \mathcal{E}^2$,

$$\dot{\mathcal{E}} = \{\mathcal{E}, H_K\} = \sqrt{\frac{\mathcal{E}}{E^x E^y}} (XE^x + YE^y).$$

or the vanishing of the (relative) momentum conjugate to length,

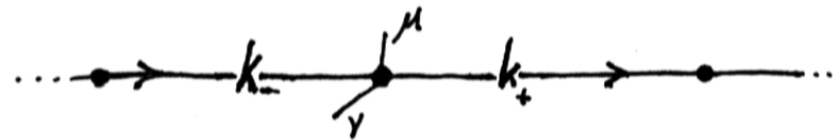
$$\frac{p_\ell}{\ell} = XE^x + YE^y.$$

Plane gravitational waves: Loop quantization



Kinematics is straightforward:

- Gauge invariant states based on simple line graph G with vertices v and labels μ, ν, k . Denoted $|\vec{v}\rangle = |v, \mu, \nu, k\rangle$.



- Geometric quantities on atom of geometry
Length

$$\hat{l} |\vec{v}\rangle = \frac{\sqrt{\gamma} l_P}{\sqrt{2}} \sqrt{|\mu| |\nu|} \left(\sqrt{|k_+ + k_- + 1|} - \sqrt{|k_+ + k_- - 1|} \right) |\vec{v}\rangle$$

Volume

$$\hat{V} |\vec{v}\rangle = \frac{\gamma^{\frac{3}{2}} l_P^3}{4} \sqrt{|\mu| |\nu| |k_+ + k_-|} |\vec{v}\rangle$$



Quantization: Flat space



For no-wave state could set k 's constant and impose $\mathcal{K} = XE^x + YE^y = 0$.

But simple quantization $\hat{\mathcal{K}} \sum_{\vec{\nu}} a_{\vec{\nu}} |\vec{\nu}\rangle = 0$ yields divergent expectation values for length of atom of geometry so, we formulate a Hermitian operator

$$\hat{\mathcal{K}}[I] = 4 \int_I dz \hat{V}^2 \left(\sqrt{\hat{E}^x} \frac{\text{Tr} [\tau_x \hat{h}_x^{-1}[I]]}{\mu_0} \sqrt{\hat{E}^x} + \sqrt{\hat{E}^y} \frac{\text{Tr} [\tau_y \hat{h}_y^{-1}[I]]}{\nu_0} \sqrt{\hat{E}^y} \right) \hat{V}^2$$

that has explicit solutions, e.g. for constant k

$$a_{\vec{\nu}} = \begin{cases} \frac{2\sqrt{3}}{(\pi\mu\nu)^2} & [\mu]_2 = 1 = [\nu]_2 \\ 0 & \text{Otherwise} \end{cases}$$

However, dynamics gives ...

Quantization: Hamiltonian constraint



With unit lapse the action of the Hamiltonian constraint is

$$\begin{aligned}
 \hat{H} |G\rangle = & -f(\vec{v}) |G\rangle + \dots + \frac{l_P}{8\gamma^{\frac{3}{2}} \mu_0 \nu_0} \sqrt{\mu\nu} \left(\sqrt{k_- + k_+ + 1} - \sqrt{k_- + k_+ - 1} \right) \left(|G, \mu_V + 2\mu_0, \nu_V - 2\nu_0\rangle \right. \\
 & + |G, \mu_V - 2\mu_0, \nu_V + 2\nu_0\rangle - |G, \mu_V + 2\mu_0, \nu_V + 2\nu_0\rangle - |G, \mu_V - 2\mu_0, \nu_V - 2\nu_0\rangle \left. \right) \\
 & + \frac{l_P}{32\gamma^{\frac{3}{2}} \mu_0 \nu_0} \sum_V \sqrt{|\mu_V| |k_+ + k_-|} \left(\sqrt{\nu_V + \nu_0} - \sqrt{\nu_V - \nu_0} \right) \left[|G, \mu_V + \mu_0, k_+ + 1, \mu_{V+1} - \mu_0\rangle \right. \\
 & - |G, \mu_V + \mu_0, k_+ + 1, \mu_{V+1} + \mu_0\rangle + |G, \mu_V + \mu_0, k_+ - 1, \mu_{V+1} + \mu_0\rangle - |G, \mu_V + \mu_0, k_+ - 1, \mu_{V+1} - \mu_0\rangle \\
 & + |G, \mu_V - \mu_0, k_+ + 1, \mu_{V+1} - \mu_0\rangle - |G, \mu_V - \mu_0, k_+ + 1, \mu_{V+1} + \mu_0\rangle + |G, \mu_V - \mu_0, k_+ - 1, \mu_{V+1} + \mu_0\rangle \\
 & - |G, \mu_V - \mu_0, k_+ - 1, \mu_{V+1} - \mu_0\rangle - |G, \mu_V + \mu_0, k_- + 1, \mu_{V-1} - \mu_0\rangle + |G, \mu_V + \mu_0, k_- + 1, \mu_{V-1} + \mu_0\rangle \\
 & - |G, \mu_V + \mu_0, k_- - 1, \mu_{V-1} + \mu_0\rangle + |G, \mu_V + \mu_0, k_- - 1, \mu_{V-1} - \mu_0\rangle - |G, \mu_V - \mu_0, k_- + 1, \mu_{V-1} - \nu_0\rangle \\
 & + |G, \mu_V - \mu_0, k_- + 1, \mu_{V-1} + \mu_0\rangle - |G, \mu_V - \mu_0, k_- - 1, \mu_{V-1} + \mu_0\rangle \left. \right] + \frac{l_P}{32\gamma^{\frac{3}{2}} \mu_0 \nu_0} \sum_V \sqrt{|\mu_V| |k_+ + k_-|} \left(\sqrt{\nu_V + \nu_0} - \sqrt{\nu_V - \nu_0} \right) \\
 & \times \left[|G, \mu_V + \mu_0, k_+ + 1, \mu_{V+1} - \mu_0\rangle - |G, \mu_V + \mu_0, k_+ + 1, \mu_{V+1} + \mu_0\rangle \right. \\
 & + |G, \mu_V + \mu_0, k_+ - 1, \mu_{V+1} + \mu_0\rangle - |G, \mu_V + \mu_0, k_+ - 1, \mu_{V+1} - \mu_0\rangle + |G, \mu_V - \mu_0, k_+ + 1, \mu_{V+1} - \mu_0\rangle \\
 & - |G, \mu_V - \mu_0, k_+ + 1, \mu_{V+1} + \mu_0\rangle + |G, \mu_V - \mu_0, k_+ - 1, \mu_{V+1} + \mu_0\rangle - |G, \mu_V - \mu_0, k_+ - 1, \mu_{V+1} - \mu_0\rangle \\
 & - |G, \mu_V + \mu_0, k_- + 1, \mu_{V-1} - \mu_0\rangle + |G, \mu_V + \mu_0, k_- + 1, \mu_{V-1} + \mu_0\rangle - |G, \mu_V + \mu_0, k_- - 1, \mu_{V-1} + \mu_0\rangle \\
 & + |G, \mu_V + \mu_0, k_- - 1, \mu_{V-1} - \mu_0\rangle - |G, \mu_V - \mu_0, k_- + 1, \mu_{V-1} - \nu_0\rangle + |G, \mu_V - \mu_0, k_- + 1, \mu_{V-1} + \mu_0\rangle \\
 & \left. - |G, \mu_V - \mu_0, k_- - 1, \mu_{V-1} + \mu_0\rangle + |G, \mu_V - \mu_0, k_- - 1, \mu_{V-1} - \mu_0\rangle \right] + \dots
 \end{aligned}$$

The ... are terms acting on the vertices other than a vertex and its nearest neighbors.



Quantization: Hamiltonian constraint



Looking for solutions of the general form

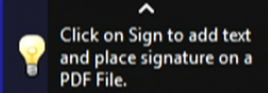
$$\hat{H}[N] \sum_{\vec{\nu}} a_{\vec{\nu}} |\vec{\nu}\rangle = 0$$

yields recursion relations...

Results (preliminary):

- The constraint recurrence relations derived from the Hamiltonian do not admit any normalizable, non-degenerate solutions where non-vanishing coefficients $a_{\vec{\nu}}$ are restricted to a bounded interval in any of the three parameters μ , ν , or k .
- Requiring any of the three quantum numbers to be constant on all vertices or edges (that is, requiring that all the k values on all edges be equal, for instance) also does not yield any normalizable, non-degenerate solutions.

Summary



Wish to determine the physical effects of discrete spatial geometry in a midi-space model.

So far,

- Classical analysis including first class constraints for reduced system (with structure functions)
- Quantization of kinematics
- Initial investigation of quantum constraints
- Uncertainty of geometric quantities and flat space constraints.

Further work:

- Further work on physical states
- Investigate the algebra of quantum constraints
- Characterize physical state space
- Investigate the propagation of "low amplitude" gravitational waves and the dispersion relations.